

Iron(II) Catalysis in Oxidation of Hydrocarbons with Ozone in Acetonitrile

Hajem Bataineh, Oleg Pestovsky and Andreja Bakac**

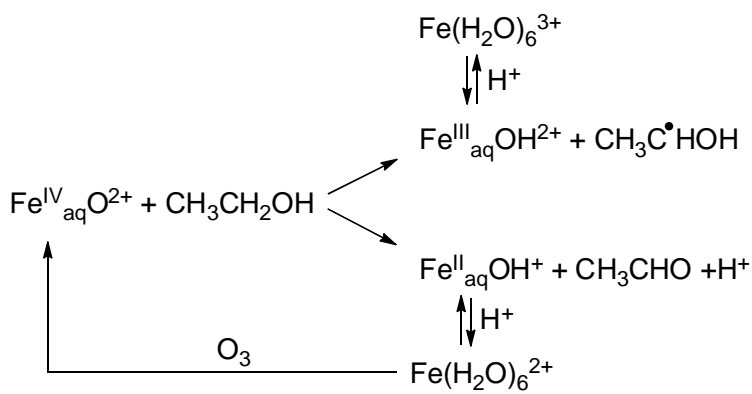
Ames Laboratory and Chemistry Department, Iowa State University, Ames, IA 50011

Email: bakac@iastate.edu, pvp@iastate.edu

Abstract Oxidation of alcohols, ethers, and sulfoxides by ozone in acetonitrile is catalyzed by sub-millimolar concentrations of $\text{Fe}(\text{CH}_3\text{CN})_6^{2+}$. The catalyst provides both rate acceleration and greater selectivity toward the less oxidized product. For example, $\text{Fe}(\text{CH}_3\text{CN})_6^{2+}$ -catalyzed oxidation of benzyl alcohol yields benzaldehyde almost exclusively (>95%) whereas uncatalyzed reaction generates a 1:1 mixture of benzaldehyde and benzoic acid. Similarly, aliphatic alcohols are oxidized to aldehydes/ketones, cyclobutanol to cyclobutanone, and diethyl ether to a 1:1 mixture of ethanol and acetaldehyde. The kinetics of oxidation of alcohols and diethyl ether are first order in $\text{Fe}(\text{CH}_3\text{CN})_6^{2+}$ and ozone, and independent of [Substrate] at concentrations greater than ~5 mM. In this regime, the rate constant for all of the alcohols is approximately the same, $k_{\text{cat}} = (8 \pm 1) \times 10^4 \text{ M}^{-1} \text{ s}^{-1}$, and that for $(\text{C}_2\text{H}_5)_2\text{O}$ is $(5 \pm 0.5) \times 10^4 \text{ M}^{-1} \text{ s}^{-1}$. In the absence of substrate, $\text{Fe}(\text{CH}_3\text{CN})_6^{2+}$ reacts with O_3 with $k_5 = (9.3 \pm 0.3) \times 10^4 \text{ M}^{-1} \text{ s}^{-1}$. The similarity between the rate constants k_5 and k_{cat} strongly argues for $\text{Fe}(\text{CH}_3\text{CN})_6^{2+}/\text{O}_3$ reaction as rate determining in catalytic oxidation. The active oxidant produced in $\text{Fe}(\text{CH}_3\text{CN})_6^{2+}/\text{O}_3$ reaction is suggested to be an Fe(IV) species in analogy with a related intermediate in aqueous solutions. This assignment is supported by the similarity in kinetic isotope effects and relative reactivities of the two species toward substrates.

Introduction

Previous studies from this group^{1,2} and others^{3,4} have established that the reaction of $\text{Fe}(\text{H}_2\text{O})_6^{2+}$ with ozone generates an iron(IV) species best described as $\text{Fe}^{\text{IV}}(\text{H}_2\text{O})_5\text{O}^{2+}$ (hereafter $\text{Fe}_{\text{aq}}\text{O}^{2+}$) on the basis of spectroscopic evidence, chemical reactivity and DFT calculations.^{1,2,5} Oxidations with $\text{Fe}_{\text{aq}}\text{O}^{2+}$ take place by oxygen atom transfer to e. g. sulfoxides and phosphines, and by hydride and hydrogen atom abstraction from C-H bonds.¹ In reactions with alcohols, aldehydes and ethers the latter two mechanisms operate in parallel, Scheme 1. The hydride path is catalytic as it generates $\text{Fe}(\text{H}_2\text{O})_6^{2+}$ which can be reoxidized to $\text{Fe}_{\text{aq}}\text{O}^{2+}$. Overall, however, the catalytic efficiency is poor because of the loss of iron as $\text{Fe}(\text{H}_2\text{O})_6^{3+}$ in the parallel one-electron (hydrogen atom transfer) path.



Scheme 1

In the reaction between $\text{Fe}(\text{H}_2\text{O})_6^{2+}$ and H_2O_2 (Fenton reaction) the reactive intermediate changes from hydroxyl radicals in acidic solutions to an iron(IV) species at near neutral pH.⁶ Such a major mechanistic change caused by a modest change in reaction conditions led us to consider the effect of other parameters, including solvent, on reactions involving solvento iron species in oxidation states 2+ to 4+. Specifically, the much higher reduction potential of the Fe(III)/Fe(II) couple in acetonitrile^{7,8} as compared to that in water suggests that the preference

for two-electron pathways of a hypothetical iron(IV) species might be greater in acetonitrile. To explore this possibility and its potential consequences for iron-catalyzed oxidations, we initiated a study of the reaction of $\text{Fe}(\text{CH}_3\text{CN})_6^{2+}$ with O_3 in acetonitrile in the presence of oxidizable substrates.⁹ The results are described herein.

Experimental

The following chemicals were obtained commercially and used as received: iron(II) perchlorate hydrate $\text{Fe}(\text{ClO}_4)_2 \cdot x\text{H}_2\text{O}$ (98%), deuterium oxide D_2O (99.9 atom %D), 1,10-phenanthroline (99+ %), benzyl alcohol anhydrous (99.8%), cyclobutanol (99+%) (all Aldrich), dimethyl sulfoxide ($\geq 99.9\%$, A.C.S spectrophotometric grade) and cyclopentanol (99%) (both Sigma-Aldrich), 2-propanol (99.9% certified ACS), tetrahydrofuran (99.9% HPLC grade), and ethyl ether anhydrous (99.9% certified ACS) (all Fisher scientific), acetonitrile- d_3 (99.8 atom % D) (Cambridge Isotope Laboratories, Inc), acetonitrile (low water content (~ 10 ppm) for HPLC, GC and spectrophotometry, Honeywell - Burdick & Jackson), 2-propanol- d_1 (99.8 atom % D) and 2-propanol- d_8 (99.9 atom % D) (both CDN Isotopes), benzyl- α, α - d_2 alcohol (98 atom % D, ISOTEC). Iron(II) bis(acetonitrile)bis(triflate) $\text{Fe}(\text{OTf})_2(\text{CH}_3\text{CN})_2$ was synthesized according to a literature procedure.¹⁰

In experiments designed to explore the effect of water on products and kinetics, anhydrous iron(II) triflate was used instead of hydrated iron(II) perchlorate. Deuterated acetonitrile was dried over 4A molecular sieves until the HDO/ H_2O signal disappeared in the ^1H NMR spectrum.

UV-Vis absorbance measurements and kinetic studies used a Shimadzu UV-3101 PC spectrophotometer and Olis RSM-1000 stopped-flow at 24.9 ± 0.1 °C. ^1H NMR spectra were recorded with a 400 MHz Bruker DRX-400 or 600 MHz Bruker Avance III spectrometer at room temperature. Waters GCT accurate mass time-of-flight mass spectrometer in positive EI mode

(70 eV) with a scan rate of 0.3 seconds per scan and a mass range of 10–200 Daltons was used to qualitatively detect some of the products. Waters MassLynx 4.0 software was used to acquire and process GC-MS data. Ozone was generated in an Ozonology L-100 ozone generator. Oxygen concentration was measured using Hanna Edge dissolved oxygen meter.

Procedures. Stock solutions of iron(II) perchlorate in CH₃CN or CD₃CN were prepared fresh before each set of experiments and standardized with phenanthroline after dilution with H₂O and using $\epsilon = 1.14 \times 10^4 \text{ M}^{-1} \text{ cm}^{-1}$ for Fe(phen)₃²⁺ at 510 nm. A correction was applied for the absorbance of iron(III)-phenanthroline as previously described.¹ Ozone solutions were prepared by continuous bubbling of ozone through CH₃CN or CD₃CN for >5 min at room temperature and diluted to the desired concentration. The concentration of ozone in stock solutions was typically 5.6±0.1 mM as determined spectrophotometrically at 260 nm, $\epsilon_{260} = 3350 \text{ M}^{-1} \text{ cm}^{-1}$. These solutions always contained residual oxygen, typically about 5.9 mM, as described below?

To determine the amount of oxygen generated in the Fe(CH₃CN)₆²⁺ /O₃ reaction in the presence and absence of substrates, the reactants were mixed rapidly in an air-free, tightly sealed vial, leaving only minimal head space to avoid equilibration between the solution and gas phases. A sample (0.5-1.0 mL) was withdrawn and injected into another sealed vial containing a dissolved oxygen electrode immersed in 18 mL of air-free water. The measurement was completed in about 40 seconds after injection. The measured value was corrected for the concentration of residual oxygen, typically around 5.9 mM in ozone stock solutions as determined after removal of O₃ with excess fumaric or maleic acid.¹¹ The same procedure was used to determine the concentration of O₂ in O₂-saturated acetonitrile. The value obtained, 11.3 mM, is in acceptable agreement with the value reported for air-saturated acetonitrile, 2.42 mM.¹²

Except in experiments specifically designed to explore the effect of O₂ on kinetics and products, solutions of iron(II) and substrates were prepared and handled anaerobically. However, since some O₂ was present in stock solutions of ozone, see above, and since the Fe(CH₃CN)₆²⁺ /O₃ reaction itself produces O₂, none of the reaction solutions were completely air-free.

Competition experiments. A solution containing known concentrations of Fe(II) and two or three substrates were mixed with ozone in a UV cell. After the disappearance of ozone at 260 nm, the products were quantified by ¹H NMR. In all of the experiments the substrate concentrations were sufficiently large to make the kinetics of each individual reaction fall into the plateau region, see Results. Product yields for benzyl alcohol, which absorbs too strongly in the UV for direct kinetic measurements, were shown independently to remain unchanged at [PhCH₂OH]₀ ≥ 4 mM. Similar experiments were conducted on mixtures of protiated and fully or partially deuterated substrates to determine kinetic isotope effects. Product yields derived from fully deuterated substrates (diethyl ether-d₁₀ and 2-propanol-d₈) were estimated as a difference between the total amount of products for the same competition observed with protiated compounds and the amount of product derived from the competing protiated substrate.

Kinetic data were obtained by monitoring the disappearance of ozone at 260 nm (Shimadzu) or in the 260-280 nm spectral range (Olis RSM-1000 Rapid Scan). In stopped flow experiments, a mixture of Fe(CH₃CN)₆²⁺ and substrate was placed in one syringe, and ozone in the other. Experiments designed to study the effect of [substrate] used 0.06-0.15 mM ozone, 0.025 mM Fe(CH₃CN)₆²⁺ and 1-50 mM substrate. The effect of [Fe(CH₃CN)₆²⁺] was explored at 0.08-0.12 mM ozone, 0.005-0.1 mM Fe(CH₃CN)₆²⁺ and 2-50 mM substrate.

Kinetic traces were fitted to an expression for first order kinetics with Kaleidagraph v4.0 or with OLIS Global-Works v2.0.190. ^1H NMR and GC-MS analyses were initiated within 5-15 min after completion of the reaction. 10% D_2O (v/v) was added to some NMR solutions to shift the interfering water peak.

Results

The UV spectrum after completion of the reaction between 1.1 mM benzyl alcohol and 0.22 mM ozone in acetonitrile exhibits a double feature in the 230-250 nm range, Figure 1, consistent with a mixture of benzaldehyde (λ_{max} 244 nm) and benzoic acid (λ_{max} 227 nm). The individual spectra are shown in Fig S1. This assignment was confirmed by ^1H NMR, Figure S2. The reaction with ozone also produced hydrogen peroxide, as shown by ^1H NMR signal at 8.56 ppm.

When the same reaction was conducted in the presence of 0.011 mM $\text{Fe}(\text{CH}_3\text{CN})_6^{2+}$, benzaldehyde was the major product detected by UV (Fig 1), ^1H NMR (Fig 2), and GC-MS. Small amounts of benzoic acid (~10%) were also observed, some of it possibly generated by oxidation of benzaldehyde with O_2 during sample manipulation. The combined yield of PhCHO and PhCOOH, based on initial ozone concentration, was 85%.

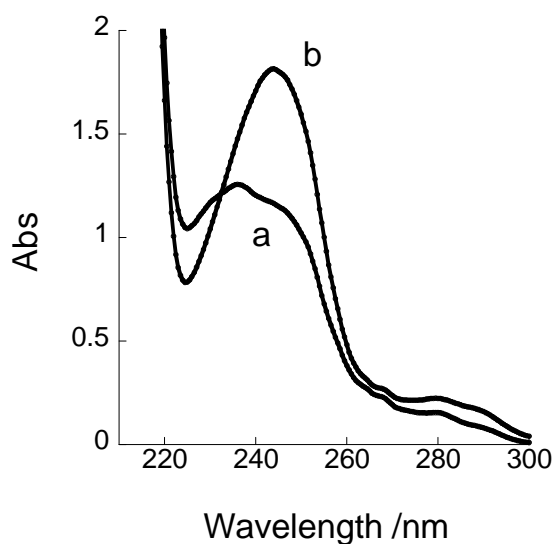


Figure 1. UV spectra of the products of the reaction between (a) 1.1 mM PhCH₂OH and 0.22 mM O₃, and (b) 1.1 mM PhCH₂OH and 0.3 mM O₃/0.011 mM Fe(CH₃CN)₆²⁺.

Fe(CH₃CN)₆²⁺-catalyzed oxidation of cyclobutanol by O₃ (1.8 mM) produced 1.55 mM cyclobutanone, Figure S3. No ring-opened products were observed by either ¹H NMR or GC-MS, ruling out a significant contribution from a path involving cyclobutanol radicals.¹ The latter are subject to rapid ring opening that ultimately yields an aldehyde(s). At the end of the reaction, about 80% of iron was still present as Fe(II).

Similarly, ethanol was oxidized to acetaldehyde, Figure S4, 2-propanol to acetone, and cyclopentanol to cyclopentanone. The results are summarized in Table 1. Product yields varied from 70% (acetaldehyde) to 85% (cyclopentanone). ¹H NMR of the products of ethanol oxidation exhibits additional signals at 8.03 and 4.64 ppm, consistent with small amounts of formic acid and acetal which are common overoxidation products of ethanol.¹³ The yields of these products increase somewhat with increasing [O₃]/[EtOH] ratio.

Table 1. Product Yields in Fe(CH₃CN)₆²⁺-Catalyzed Oxidation of Alcohols, DMSO and Et₂O by Ozone

Substrate (mM)	[O ₃]/mM	[Fe(CH ₃ CN) ₆ ²⁺]/mM	Major Product	% Yield
dimethyl sulfoxide (9.6)	1.9	0.028	dimethyl sulfone	100
diethyl ether (8.5)	1.2	0.052	(ethanol + acetaldehyde)	100
cyclopentanol (9.8)	1.4	0.024	cyclopentanone	85
cyclobutanol (9.6)	1.8	0.025	cyclobutanone	85
2-propanol (32)	0.1	0.025	acetone	80
ethanol (21.1)	0.83	0.055	acetaldehyde	70
benzyl alcohol (10)	1.8	0.048	benzaldehyde	70

The reaction with diethyl ether produced a 1:1 mixture of C₂H₅OH and CH₃CHO in 100% yield, Figure S5. Dimethyl sulfoxide (DMSO) was oxidized to the sulfone, also in 100% yield, Figure S6. At an initial Fe(CH₃CN)₆²⁺ concentration of >0.020 mM, the majority (70-90%) of iron was still present as Fe(II) at the end of the reactions listed in Table 1 provided the concentration of substrate exceeded ~5 mM. At much lower initial concentrations of Fe(CH₃CN)₆²⁺ and substrate, up to 40-60 % of Fe(CH₃CN)₆²⁺ was oxidized to Fe(III).

Fe(CH₃CN)₆²⁺-catalyzed oxidation of THF by O₃ yielded several products as shown by GC-MS and ¹H NMR, Figures 2 and S7. On the basis of mass spectra, the GC peak at 4.42 min is assigned to an equilibrated mixture¹⁴ of 2-hydroxytetrahydrofuran (2-OH-THF) and 4-hydroxybutanal, and that at 6.18 min to γ -butyrolactone. All three species were clearly identified and quantified by ¹H NMR, Figure S7. The combined yield is 75% (in 4:2:1 ratio, respectively). Also observed in the ¹H NMR are small amounts of formic acid which was also found in previous studies of THF oxidation.¹⁵ Several other small peaks were not identified. The products eluting at 9-10 min in Figure 2 are attributed to THF dimers and condensation products as deduced from mass spectral data. These products are also formed upon electrochemical oxidation of THF in aqueous sulfuric acid.¹⁵

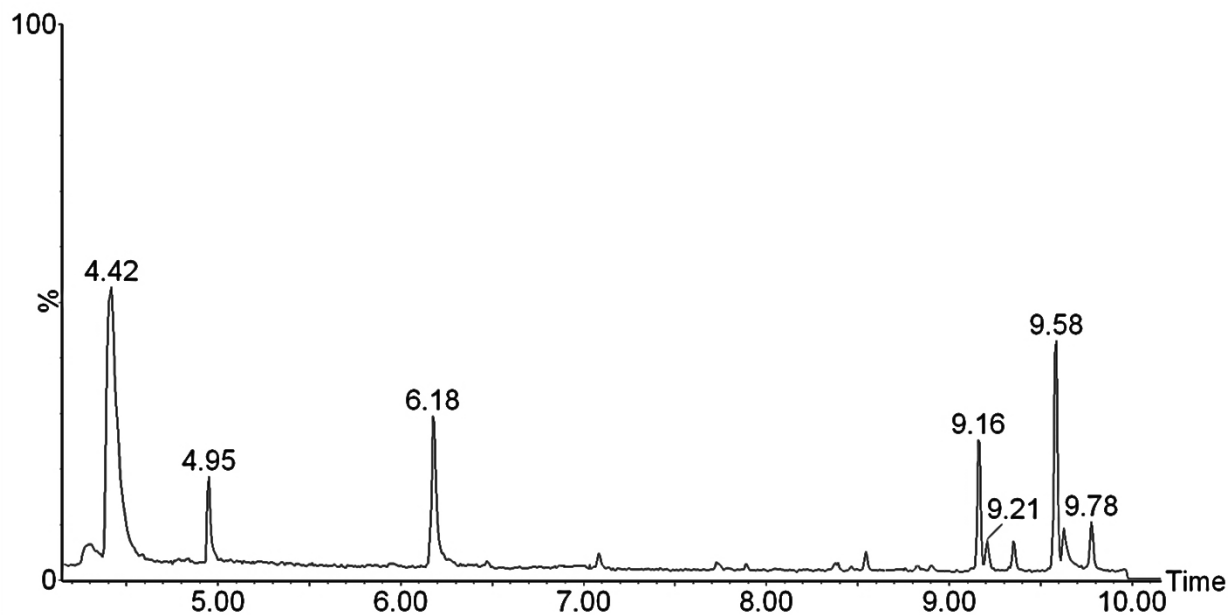


Figure 2. Gas chromatogram of products obtained by oxidation of 5.6 mM THF by 1.35 mM $O_3/0.1$ mM Fe(II).

The overall picture of THF oxidation changes dramatically when an alcohol is added as co-substrate. As shown on the example of THF/ benzyl alcohol mixture, Figures S8-S10, the main products (>90%) are the acetal 2-OR-THF and aldehyde/ketone derived from the alcohol. THF oxidation products, i. e. hydroxytetrahydrofuran/4-hydroxybutanal and γ -butyrolactone, accounted for only 5% of products.

In search of the source of 2-OR-THF we considered the known reaction¹⁶ between alcohols and 4-hydroxybutanal, the latter being one of THF oxidation products. This reaction generates 2-OR-THF in the presence of an acid catalyst at 20-100° C,¹⁶ but is extremely slow (about 17 hours) under our experimental conditions. Also, no new products were generated upon mixing alcohols with product solutions of $Fe(CH_3CN)_6^{2+}/O_3/THF$ reaction. A slow overnight reaction between alcohols and THF in the presence of $Fe(CH_3CN)_6^{2+}$ (0.5 mM) did produce 2-OR-THF when the concentrations of alcohols (60 mM) and THF (80 mM) were about ten-fold higher than

is typical in our work. Clearly, the rapid (several seconds) formation of 2-OR-THF under our standard catalytic conditions utilizes a different path and must involve an intermediate(s) generated in the course of the $\text{Fe}(\text{CH}_3\text{CN})_6^{2+}/\text{O}_3$ oxidation of THF and/or alcohol. Since close to 100% of iron was still present as Fe(II) at the end of the $\text{Fe}(\text{CH}_3\text{CN})_6^{2+}/\text{O}_3/\text{THF/alcohol}$ it is clear that the products were either formed in a series of 2-e steps or that Fe(III), if involved, was re-reduced to Fe(II) by reaction intermediate(s).

Kinetics. Substrates (5-50 mM) were used in large excess over ozone (0.06-0.15 mM) and $\text{Fe}(\text{CH}_3\text{CN})_6^{2+}$. The loss of ozone was monitored at 260 nm. Kinetic traces in the plateau region, see below, were exponential and yielded pseudo-first-order rate constants k_{obs} .

Ozone oxidation of organic substrates used in this work is slow but not negligible in comparison with the $\text{Fe}(\text{CH}_3\text{CN})_6^{2+}$ -catalyzed reaction. The rate law for the disappearance of ozone is thus given by eq 1, where k_{cat} represents the rate constant for the catalytic reaction of eq 2, k_{O_3} is the independently-determined rate constant for the direct O_3 /substrate reaction, Table S1, and S is substrate. The contribution from direct reaction to k_{obs} was typically <10%, but increased as substrate concentrations increased and Fe(II) concentrations decreased. In the least favorable case (50 mM 2-PrOH at 0.025 mM Fe(II)), this contribution was 20%. The use of higher concentrations of the catalyst, which would benefit the catalytic reaction, was not feasible because the reaction became too fast and signal-to-noise ratio poor.

$$-d[\text{O}_3]/dt = k_{\text{O}_3}[\text{O}_3][\text{S}] + k_{\text{cat}}[\text{O}_3] [\text{Fe}(\text{CH}_3\text{CN})_6^{2+}]^m [\text{S}]^n = k_{\text{obs}} [\text{O}_3] \quad (1)$$



The experimentally determined k_{obs} was corrected for the direct path to give k_{corr} , eq 3.

$$k_{\text{corr}} = k_{\text{obs}} - k_{\text{O}_3}[\text{S}] = k_{\text{cat}} [\text{Fe}(\text{CH}_3\text{CN})_6^{2+}]^m [\text{S}]^n \quad (3)$$

The reaction is first order in $[\text{Fe}(\text{CH}_3\text{CN})_6^{2+}]$ ($m = 1$) as shown by linear dependence of k_{corr} on $[\text{Fe}(\text{CH}_3\text{CN})_6^{2+}]$ at two different concentrations of 2-PrOH in Figure 3. First order dependence on $[\text{Fe}(\text{CH}_3\text{CN})_6^{2+}]$ holds for all of the substrates examined.

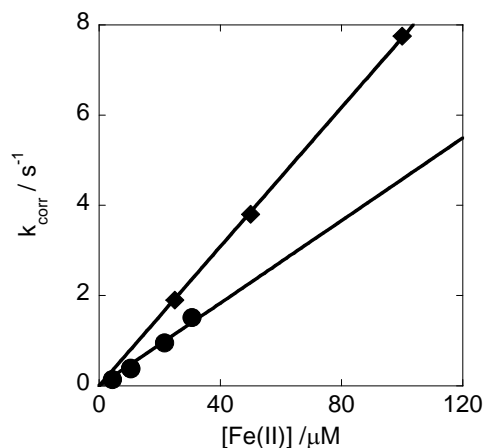


Figure 3. Plot of k_{corr} vs concentration of $\text{Fe}(\text{CH}_3\text{CN})_6^{2+}$ for the catalytic oxidation of 2-PrOH with ozone (0.08-0.12 mM.). Concentrations of 2-PrOH are 2 mM (circles) and 50 mM (squares).

The dependence on $[\text{2-PrOH}]$, on the other hand, is quite modest as shown by the small difference in slopes of the two lines in Figure 3, i. e. $3.6 \times 10^4 \text{ M}^{-1}\text{s}^{-1}$ and 7.7×10^4 at $[\text{2-PrOH}] = 2 \text{ mM}$ and 50 mM , respectively. This general picture holds for other substrates as well as shown in Table S2 and illustrated by the plot of k_{corr} vs $[\text{Substrate}]$ in Figure 4.

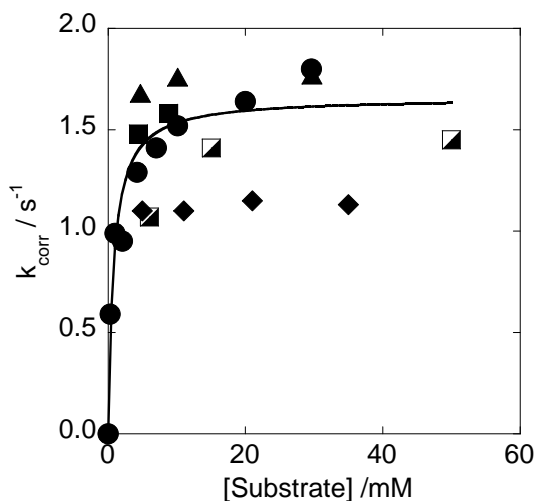


Figure 4. Plot of k_{corr} against substrate concentration for $\text{Fe}(\text{CH}_3\text{CN})_6^{2+}$ -catalyzed oxidations with ozone of 2-propanol (circles), ethanol (half-filled squares), THF (squares), cyclobutanol (triangles) and diethyl ether (diamonds). All experiments have $[\text{Fe}(\text{CH}_3\text{CN})_6^{2+}]_0 = 0.025 \text{ mM}$, $[\text{O}_3] = 0.06\text{-}0.15 \text{ mM}$.

After the sharp initial rise, the rate constants in Figure 4 reach an approximately constant value of $1.5 \pm 0.2 \text{ s}^{-1}$ for most substrates, and 1.1 s^{-1} for diethyl ether. The initial concentration of $\text{Fe}(\text{CH}_3\text{CN})_6^{2+}$ in these experiments was approximately constant at $0.025 \pm 0.002 \text{ mM}$. After the reaction, $\sim 80\%$ of $\text{Fe}(\text{CH}_3\text{CN})_6^{2+}$ was recovered in the plateau region in Figure 4, but only about 50% in the rising portion at low substrate concentrations. Also, the fit to exponential kinetics at low [substrate] was poor, and only the initial 50% of reaction was used to evaluate the rate constants.

In the plateau region the reaction is clearly catalytic in $\text{Fe}(\text{CH}_3\text{CN})_6^{2+}$ and the rate law is reasonably well approximated by eq 4 (i. e. n of eq 2 is zero), yielding $k_{\text{cat}} = k_{\text{corr}}/[\text{Fe}(\text{CH}_3\text{CN})_6^{2+}] = (5 \pm 0.5) \times 10^4 \text{ M}^{-1} \text{ s}^{-1}$ for Et_2O and $(8 \pm 1) \times 10^4 \text{ M}^{-1} \text{ s}^{-1}$ for the remaining substrates.

$$-d[\text{O}_3]/dt = d[\text{Product}]/dt = k_{\text{cat}}[\text{Fe}(\text{CH}_3\text{CN})_6^{2+}][\text{O}_3] = k_{\text{corr}} [\text{O}_3] \quad (4)$$

The kinetic behavior of DMSO is qualitatively similar to that of alcohols and ethers, but the rate constant is much larger, reaching a saturation value of $39 \pm 1 \text{ s}^{-1}$ at 0.025 mM Fe(II), Figure 5. This result implies much greater reactivity of $\text{Fe}(\text{DMSO})_n(\text{CH}_3\text{CN})_{6-n}^{2+}$ complex(es)^{17,18} compared to $\text{Fe}(\text{CH}_3\text{CN})_6^{2+}$. The support for $\text{Fe}(\text{DMSO})_n(\text{CH}_3\text{CN})_{6-n}^{2+}$ in this work comes from the observation of broadened ¹H NMR methyl resonances of DMSO in CD₃CN in the presence of Fe(II), consistent with an exchange between free and complexed DMSO. As expected, the signal sharpens upon addition of D₂O (15%, v/v) which leads to dissociation of DMSO.

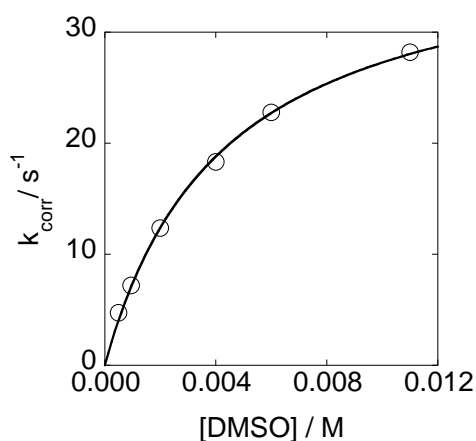
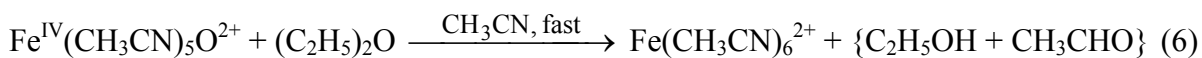
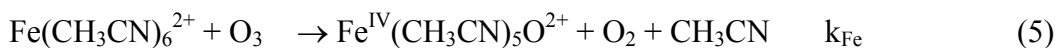


Figure 5. Plot of k_{obs} vs [DMSO] for the reaction with O_3 (0.1 mM) / $\text{Fe}(\text{CH}_3\text{CN})_6^{2+}$ (0.025 mM).

Kinetic measurements for the $\text{Fe}(\text{CH}_3\text{CN})_6^{2+} / \text{O}_3$ reaction in the absence of substrates and with $\text{Fe}(\text{CH}_3\text{CN})_6^{2+}$ in large excess yielded $k_{\text{obs}} = 20 \text{ s}^{-1}$ at $[\text{Fe}(\text{CH}_3\text{CN})_6^{2+}]_0 = 0.21 \text{ mM}$, and 29 s^{-1} at $[\text{Fe}(\text{CH}_3\text{CN})_6^{2+}]_0 = 0.30 \text{ mM}$, which results in $k_{\text{Fe}} = (9.3 \pm 0.3) \times 10^4 \text{ M}^{-1} \text{ s}^{-1}$, eq 5. The similarity between the rate constants k_5 and k_{cat} strongly argues that they apply to the same reaction, i. e. formation of an intermediate, presumably $\text{Fe}^{\text{IV}}(\text{CH}_3\text{CN})_5\text{O}^{2+}$ (hereafter $\text{Fe}^{\text{IV}}_{\text{AN}}\text{O}^{2+}$), see later, or a related species in analogy with $\text{Fe}^{\text{IV}}_{\text{aq}}\text{O}^{2+}$ that is produced in $\text{Fe}(\text{H}_2\text{O})_6^{2+} / \text{O}_3$

reaction in acidic aqueous solutions.¹ In this scenario, $\text{Fe}^{\text{IV}}_{\text{AN}}\text{O}^{2+}$ rapidly oxidizes substrates as in eq 6, thereby regenerating $\text{Fe}(\text{CH}_3\text{CN})_6^{2+}$ which re-enters eq 5.



Runs with excess ozone exhibited a rapid initial step followed by slower disappearance of large, nonstoichiometric amounts of ozone in a reaction apparently catalyzed by iron. The fast initial step took place on a time scale appropriate for k_{Fe} that was determined with excess $\text{Fe}(\text{CH}_3\text{CN})_6^{2+}$, but a reliable rate constant could not be extracted under those conditions.

In several experiments the concentration of O_2 was determined at the end of reaction with use of dissolved oxygen electrode as described in Experimental. Under standard catalytic conditions (0.050 mM $\text{Fe}(\text{CH}_3\text{CN})_6^{2+}$, 0.8 mM O_3 , 20 mM substrate), the reactions with DMSO and with $(\text{C}_2\text{H}_5)_2\text{O}$ generated 0.9 equivalents of O_2 per O_3 , Table S3. This result, combined with quantitative product yields in Table 1, leads to the approximate stoichiometry in eq 7.



For the remaining substrates in Table 1, the net increase in O_2 content was lower, typically 0.6 equivalents per O_3 , suggesting some O_2 consumption in parallel 1-e processes, see later. When no substrates were added, the increase in O_2 was only about 0.2 equivalents per mole of O_3 regardless of whether $\text{Fe}(\text{CH}_3\text{CN})_6^{2+}$ was used in catalytic amounts or in concentrations comparable to those of O_3 (~ 0.8 mM). In both cases ozone was consumed completely, although at low iron concentrations the reaction took about 15 minutes, much longer than in the presence of added substrates. Given that O_3 persists in acetonitrile for hours in the absence of $\text{Fe}(\text{CH}_3\text{CN})_6^{2+}$, it is clear that $\text{Fe}(\text{CH}_3\text{CN})_6^{2+}$ /acetonitrile combination leads to catalytic O_3 consumption. Clearly, acetonitrile is less reactive than the substrates in Table 1. Moreover,

small amounts of $\text{Fe}(\text{CH}_3\text{CN})_6^{2+}$ remained after completion of the reaction even when ozone was in excess. In experiments with equimolar amounts of $\text{Fe}(\text{CH}_3\text{CN})_6^{2+}$ and O_3 , about 60% of $\text{Fe}(\text{II})$ remained after completion of the reaction in CH_3CN , but only traces (<5%) in CD_3CN demonstrating a large solvent kinetic isotope effect. Unfortunately, no oxidation products of CH_3CN could be detected by ^1H NMR or GC-MS owing to interference by the large solvent peaks. No formaldehyde was detected with chromotropic acid.

Effect of Fe(III), O_2 and water. There is a mild increase in product yields under oxygen-rich conditions, as shown for ethanol in Table 2. At approximately constant concentrations of $\text{Fe}(\text{CH}_3\text{CN})_6^{2+}$, O_3 , and EtOH , an increase in oxygen concentration from 1 mM to 7 mM led to an increase in acetaldehyde yield from 82% to 94%, and an increase in the recovery of $\text{Fe}(\text{CH}_3\text{CN})_6^{2+}$ from 91% to 98%. Oxygen also appears to have a mild inhibiting effect on the kinetics. The rate constant in the presence of excess O_2 (≥ 1.3 mM) is about 15% smaller than that obtained in the experiments that had only a small background concentration of O_2 (ca 0.2 mM, comparable to that of ozone), Table 3.

Externally added $\text{Fe}(\text{ClO}_4)_3$ also improves product yields. As shown in the last entry in Table 2, the yields of acetaldehyde become quantitative in the presence of 0.24 mM $\text{Fe}(\text{III})$.

Replacing the $\text{Fe}(\text{II})$ catalyst with $\text{Fe}(\text{III})$ results in a slow initial decrease in ozone concentration, but the reaction accelerates with time suggesting a buildup of $\text{Fe}(\text{II})$ and onset of $\text{Fe}(\text{II})$ catalysis. Experiments with $\text{Fe}(\text{III})/\text{EtOH}/\text{acetonitrile}$ confirmed that $\text{Fe}(\text{II})$ was indeed produced.

Up to 100 mM of added water has no effect on product yields or catalyst recovery as shown for ethanol and 2-propanol in Table 2, but the rate constant shows a small systematic increase with increasing $[\text{H}_2\text{O}]$. At larger concentrations of H_2O , product yields and catalyst recovery

both decrease and the rate constant increases. All catalytic activity ceases when water content reaches 3% (~1.5 M). The presence of water in the coordination sphere of iron and in the solvent apparently changes the Fe(III)/Fe(II) potentials to an extent sufficient to restore the chemistry to that characteristic of aqueous solution.¹

Table 2. Effect of Fe(III) and O₂ on Ethanol Oxidation^a

[O ₂]/ mM	[Fe(III)] ₀ /mM	[CH ₃ CHO] _∞ /mM	% [Fe(II)] _∞ ^b
1		82	91
1 ^c		82	93
7		94	98
1	0.052	85	105
1	0.245	100	130

^a [Fe(CH₃CN)₆²⁺]₀ = 0.047-0.060 mM, [O₃] = 0.93-1.0 mM, [C₂H₅OH] = 43-55 mM. ^b % Fe(II) recovered at the end of reaction. ^c Added [H₂O] = 56 mM.

Table 3. Effect of H₂O on the Kinetics and Catalyst Recovery^a

[O ₃]/ mM	Substrate	Added [H ₂ O]/ mM	k _{corr} /s ⁻¹	% [Fe(II)] _∞ ^b
0.054	2-propanol	0	1.7	96
0.064	2-propanol	50	2.0	92
0.056	2-propanol	99	2.6	96
0.050	2-propanol	198	3.0	80
0.072	ethanol	0	1.4	92
0.063	ethanol	149	2.3	76
0.060	ethanol	489	4.4	64

^a Conditions: [Substrate] = 20 mM, [Fe(CH₃CN)₆²⁺]₀ = 0.025 mM.

Competition Experiments. To gain an insight into the reactivity of the catalytic intermediate, presumed to be $\text{Fe}^{\text{IV}}_{\text{AN}}\text{O}^{2+}$, competition experiments were performed with several substrates, see *Experimental*. The results (Figures S11-S16) are summarized in Table 4. The ratios of rate constants k_1/k_2 for various substrates were calculated from the expression $k_1/k_2 = [\text{P}_1][\text{S}_2]/[\text{P}_2][\text{S}_1]$, where S_1 and S_2 are two competing substrates, and P_1 and P_2 their respective products. In the experiment with three competing substrates the listed ratios are $[\text{P}_1][\text{S}_2]/[\text{P}_2][\text{S}_1]$ and $[\text{P}_2][\text{S}_3]/[\text{P}_3][\text{S}_2]$, where S_3 and P_3 stand for $(\text{CH}_3)_2\text{CHOH}$ and $(\text{CH}_3)_2\text{CO}$, respectively,.

Table 4. Results of Competition Experiments^a

O_3 /mM	Substrate (mM)	Product (mM)	k_1/k_2 ^b
0.66	benzyl alcohol (4.9) +	benzaldehyde (0.27) +	4.2
	ethanol (19)	acetaldehyde (0.25)	
0.73	benzyl alcohol (4.9) +	benzaldehyde (0.29) +	1.9
	cyclobutanol (10)	cyclobutanone (0.31)	
1.7	cyclobutanol (10) +	cyclobutanone (0.62) +	2.4
	ethanol (30)	acetaldehyde (0.76)	
0.86	cyclobutanol (10) +	cyclobutanone (0.40) +	1.3
	2-propanol (11)	acetone (0.34)	
1.0	benzyl alcohol (4.7) +	benzaldehyde (0.32) +	3.8, 0.54 ^c
	ethanol (10) +	acetaldehyde (0.18) +	
	2-propanol (9.6)	acetone (0.32)	
1.1	benzyl alcohol (4.8) +	benzaldehyde (0.49) +	1.3
	diethyl ether (4.7)	acetaldehyde / ethanol (0.37)	

^a $[\text{Fe}(\text{CH}_3\text{CN})_6] = 0.05 - 0.06$ mM. ^b Ratio of rate constants for competing substrates S_1 and S_2 in the order listed in each set. ^c Ratio of rate constants for ethanol and 2-propanol.

All of the rate constants were normalized to $k_{\text{EtOH}} = 1.0$ in Table 5. Similar experiments with deuterated substrates (Figures S17-S21) yielded the results in Table 6 from which kinetic isotope effects in Table 7 were calculated.

Table 5. Relative Rate Constants for Oxidations with $\text{Fe}^{\text{IV}}_{\text{AN}}\text{O}^{2+}$

Substrate	Average k_{rel}	$k_{\text{H}_2\text{O}}/\text{M}^{-1}\text{s}^{-1\text{a}}$
ethanol	[1.0]	2.51×10^3
2-propanol	2.0	3.22×10^3
cyclobutanol	2.2	3.13×10^3
diethyl ether	3.1	4.74×10^3
benzyl alcohol	4.0	14.2×10^3

^a Directly measured rate constants for reactions of $\text{Fe}(\text{H}_2\text{O})_5\text{O}^{2+}$ in 0.1 M aqueous HClO_4

Table 6. Products Obtained in Competition Between Protiated and Deuterated Substrates^a

O_3 /mM	Substrate (mM)	Product (mM)
1.15	diethyl ether-d10 (5.6)	acetaldehyde / ethanol (0.20) ^b
	benzyl alcohol (4.8)	benzaldehyde (0.66)
1.1	ethanol (16.6)	acetaldehyde (0.53)
	benzyl alcohol-d2 (4.7)	benzaldehyde (0.18)
0.85	2-propanol-d1 (10.1)	acetone (0.19)
	benzyl alcohol (4.8)	benzaldehyde (0.46)
1.39	cyclobutanol (9.7)	cyclobutanone (0.81)
	benzyl alcohol-d2 (9.1)	benzaldehyde (0.34)

1	2-propanol-d8 (10.3)	acetone (0.22) ^b
	benzyl alcohol (4.8)	benzaldehyde (0.54)

^a By ¹H NMR. ^b Estimated from experimentally determined amount of PhCHO and assuming a 75% cumulative yield of all products (as found with protiated substrates).

Table 7. Kinetic Isotope Effects for Reactions of Fe^{IV}_{AN}O²⁺

Substrate	k _H /k _D
diethyl ether (d ₁₀)	2.3
benzyl alcohol (d ₂)	3.8
2-propanol (d ₁ , d ₈)	2.5

Discussion

The oxidation of alcohols, ethers and sulfoxides by ozone in acetonitrile is catalyzed by Fe(CH₃CN)₆²⁺. Concentrations of Fe(CH₃CN)₆²⁺ as low as 0.02 mM are sufficient for the catalytic reaction to dominate over the uncatalyzed O₃/substrate reaction at substrate concentrations lower than about 50 mM. The catalyst not only provides rate acceleration, but also increases the selectivity toward the less oxidized product. This is illustrated in Figure 1 and Figure S2 on the example of benzyl alcohol which is oxidized to benzaldehyde in the Fe(CH₃CN)₆²⁺-catalyzed path, and to a 1:1 mixture of benzaldehyde and benzoic acid in direct oxidation with ozone.

Saturation kinetics are observed at [substrate] >5 mM (Figure 4). The rate constants reach an approximate limit of k_{cat} = (8±1) × 10⁴ M⁻¹ s⁻¹ for all of the substrates except diethyl ether which reacts somewhat more slowly, k_{cat} = (5±0.5) × 10⁴ M⁻¹ s⁻¹. The observed variations in k_{cat} can be rationalized by variations in Fe(II)-substrate binding constants and perhaps different

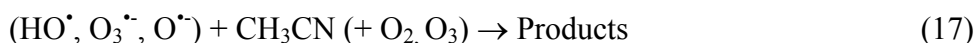
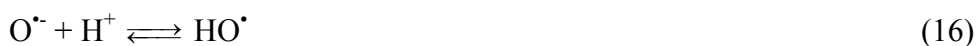
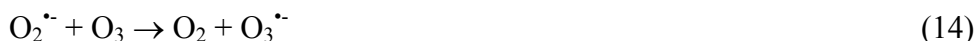
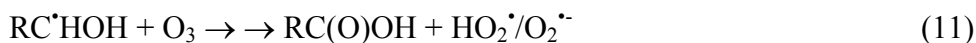
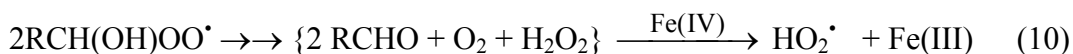
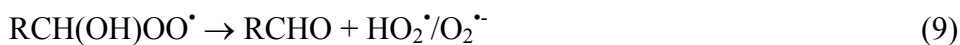
contributions from 1-e and 2-e paths, see later. The role of substrate binding is clearly seen in the reaction with DMSO which interacts strongly with $\text{Fe}(\text{CH}_3\text{CN})_6^{2+}$ and reaches $k_{\text{cat}} = 1.5 \times 10^6 \text{ M}^{-1} \text{ s}^{-1}$, Figure 5.

As the concentration of substrate drops below 5 mM, the rate constant decreases sharply, Figure 4. In this regime up to 50% of iron is oxidized to Fe(III) in the course of the reaction resulting in slower kinetics. Side reactions of Fe(IV) with $\text{Fe}(\text{CH}_3\text{CN})_6^{2+}$ and with the solvent, see later, are also most severe at low substrate concentrations, which further reduces the efficiency of the catalytic reaction. The remainder of the discussion will focus on the saturation regime.

Most efficient are the oxidations of diethyl ether and dimethyl sulfoxide. Both generate 2-electron oxidation products quantitatively, Figures S5 and S6, with only small losses ($\leq 20\%$) of the catalyst over 20-70 catalytic cycles, Table 1. These data are most easily explained by a single-step two-electron oxidation of substrates by $\text{Fe}^{\text{IV}}_{\text{AN}}\text{O}^{2+}$, eq 6, followed by regeneration of $\text{Fe}^{\text{IV}}_{\text{AN}}\text{O}^{2+}$ in reaction 5.

Product yields are somewhat lower, 70-85%, in the reactions with alcohols, Table 1. We attribute these results to a contribution from a one-electron path of eq 7 which leads to oxygen radicals ($\text{HO}^\bullet/\text{O}^\bullet$, O_3^\bullet , O_2^\bullet and others) known to be involved in chain decomposition of O_3 in aqueous solutions.¹⁹⁻²⁴ Some of the key reactions believed responsible for the loss of O_3 in this work are shown in eq 8-18, written in analogy with the chemistry in aqueous solutions and in the gas phase and supported by limited information on the reactivity of ozone and oxygen radicals in non-aqueous solvents.²⁵⁻³⁰





Hydroxyalkyl radicals generated in eq 7 react with both O_2 (eq 8) and O_3 (eq 11) and produce superoxide, a powerful reductant and nucleophile.³⁰ The reduction of Fe(III) by $\text{O}_2^{\bullet-}$,²⁴ eq 13, is the key step that regenerates Fe(II). The competing reaction between O_3 and $\text{O}_2^{\bullet-}$,³¹ the latter a well recognized chain carrier in the decomposition of ozone,^{23,32} generates $\text{O}_3^{\bullet-}$ followed by dissociation³³ to give $\text{O}^{\bullet-}$, eq 14-15. The latter may be protonated (pK_a of HO^\bullet in $\text{H}_2\text{O} = 11.9$)³⁴ if sufficient amount of water is present in the solvent, but protonation is not required for the next step since both HO^\bullet and $\text{O}^{\bullet-}$ will oxidize the solvent and/or substrate by hydrogen atom abstraction,³³ eq 17 and 18. Even though the rate constant for the reaction of HO^\bullet with acetonitrile is smaller ($k = 1.0 \times 10^6 \text{ M}^{-1} \text{ s}^{-1}$ in acetonitrile)³⁵ than the rate constants for the reactions with alcohols (e. g. $k_{\text{EtOH}} = 8.3 \times 10^7 \text{ M}^{-1} \text{ s}^{-1}$),²⁶ the concentration advantage makes the

reaction with CH₃CN about 5-10 fold faster at 20-50 mM ethanol that is typical in this work. Presumably, other radicals in eq 17-18 exhibit similar reactivity pattern and together with HO[•] lead to a loss of oxidizing equivalents and less than quantitative yields of substrate-derived products. Reaction 18 regenerates RC[•]HOH which reenters the scheme.

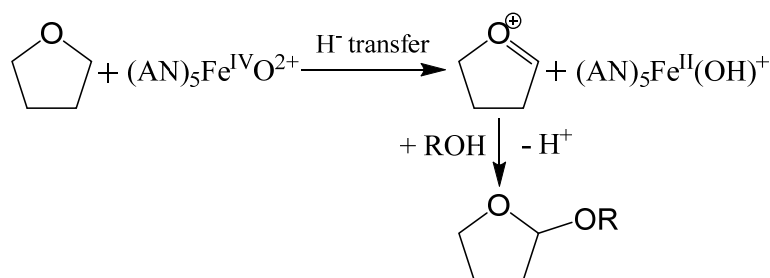
According to the above mechanism, the beneficial effect of added Fe(III) arises mainly from its efficient scavenging of O₂^{•-} in eq 12.²⁴ This step both regenerates the catalyst and minimizes the importance of reactions 14-17 which lead to the loss of O₃.

Increased product yields and somewhat slower kinetics of O₃ loss under O₂-rich conditions are also consistent with known reactivity of radicals with O₃ and O₂. At high [O₂], most of the radicals react with O₂ as in eq 8, followed by reactions 9-10 and 12-18. In the absence of externally added O₂, the concentrations of O₂ and O₃ are comparable (see Experimental), and reaction 11 becomes competitive with reaction 8 which increases the rate of ozone consumption and yields of doubly oxidized products.³⁶ Moreover, alkylperoxyl radicals produced in eq 8 also react with O₃ to generate alkoxy radicals RCH(OH)O[•], eq 19, followed by rearrangement and/or further reactions with O₂, O₃ and substrates.^{37,38}



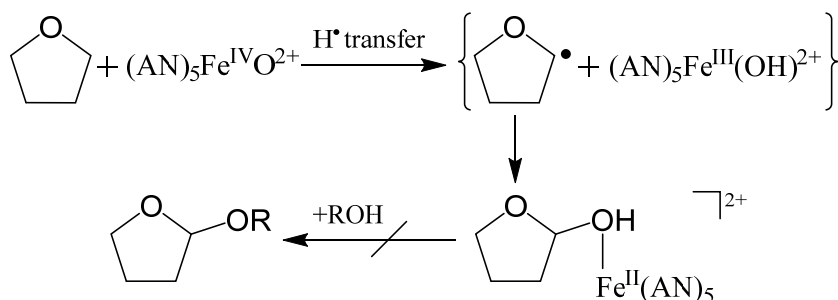
In agreement with the above scheme, the concentration of O₂ found after completion of the reactions with alcohols is significantly smaller than one would calculate by adding the amount produced from ozone in reaction 5 to the [O₂] initially present. Clearly, some O₂ is consumed in the course of alcohol oxidation. On the other hand, the concentration of O₂ found after the oxidation of DMSO and (C₂H₅)₂O is close to that calculated, supporting the notion that 1-e oxidation of these substrates is negligible. DMSO is probably oxidized by OAT, similar to the reaction in water.¹ Quantitative product yields and measurable hydrogen k_{ie} for diethyl ether

suggests hydride transfer.¹ Additional support for hydride transfer from ethers, and by inference from alcohols as well, comes from the effect of alcohols on oxidation products of THF. The formation of acetals is most reasonably explained by hydride transfer that generates an oxonium ion followed by the reaction with alcohols as shown in Scheme 1. The oxonium ion shown was proposed earlier as an intermediate in cationic polymerization of THF in the presence of triphenylmethyl cation salts.³⁹



Scheme 1.

The alternative rebound mechanism that begins with hydrogen atom transfer would generate the hemiacetal as shown in Scheme 2. This mechanism is ruled out by our observation that the hemiacetal does not react with alcohols under our conditions. In contrast to ethers, the intermediates generated in the process of alcohol oxidation by hydride transfer generate aldehydes/ketones by rapid deprotonation at oxygen.



Scheme 2.

The induction period observed in the O₃/substrate reaction when iron is initially present as Fe(III) is most easily explained by the need to reduce Fe(III) to Fe(II), presumably through a scheme involving one-electron reduction of O₃ by the substrate^{19,40} followed by eq 15-18. The complex, multistep chemistry in eq 17-18 is envisioned to generate some O₂^{•-} which reduces Fe(III) to Fe(II) and thus leads to the production of Fe^{IV}_{AN}O²⁺ via reaction 5.

The disappearance of ozone in the presence of catalytic amounts of Fe(CH₃CN)₆²⁺ in acetonitrile even in the absence of more reducing substrates shows that the solvent itself can be catalytically oxidized. It is not clear whether Fe^{IV}_{AN}O²⁺ oxidizes CH₃CN in 1-e or 2-e steps. Measurable amounts of Fe(CH₃CN)₆²⁺ found in such solutions after all of O₃ disappeared support a 2-e catalytic reaction that might take place by oxygen atom transfer or hydride transfer. On the other hand, as shown above in the reaction with alcohols, 1-e chemistry can also bring about the disappearance of ozone and formation of Fe(CH₃CN)₆²⁺. In support of one-electron route we note that aqueous ferryl(IV) reacts with CH₃CN by hydrogen abstraction and does not regenerate Fe_{aq}²⁺.¹ Also, the much smaller amount of recovered Fe(II) after completion of Fe(II)/O₃ reaction in CD₃CN indicates a large solvent isotope effect, again consistent with HAT, although hydride abstraction cannot be entirely ruled out.

Throughout this discussion it has been assumed that oxidizing intermediate is an Fe(IV) species, Fe^{IV}_{AN}O²⁺, although so far we have not been able to observe or characterize it spectroscopically. The relative reactivity toward the substrates in Table 5 appears consistent with this assignment in that the trend in acetonitrile follows closely that observed for Fe_{aq}O²⁺ in aqueous solutions. In that work it was possible to carry out direct kinetic measurements of substrate oxidation by pre-formed Fe_{aq}O²⁺. As shown in Table 5, benzyl alcohol is the most reactive among alcohols in both solvents, but the yield of 2-e oxidation product in acetonitrile is

among the lowest. This result may suggest a significant contribution from the 1-e path. Alternatively, the reaction may involve an attack by $\text{Fe}^{\text{IV}}_{\text{AN}}\text{O}^{2+}$ at the benzene ring to generate multiple products, similar to the reaction of O_3 with PhCH_2OH ,⁴¹ or reactions of other Fe(IV)-oxo complexes with aromatic compounds.^{42,43}

The kinetic isotope effect for the reaction with 2-propanol is also similar in the two solvents. The value of $k_{\text{H}}/k_{\text{D}}$ for the methine C-H is 2.5 in acetonitrile (Table 7) and 2.1 in H_2O ,¹ consistent with hydride transfer proposed previously. These results however do not rigorously rule out other potential oxidizing intermediates, such as an ozonide or Fe(III)-(CH₂CN) radical that may also react by hydride or hydrogen atom transfer.

Conclusions

Perchlorate and trifluoromethane sulfonate salts of iron(II) efficiently catalyze oxidation of alcohols and ethers with ozone in acetonitrile. This result stands in stark contrast with that obtained in acidic aqueous solutions where, under comparable conditions, all of $\text{Fe}(\text{H}_2\text{O})_6^{2+}$ is quickly oxidized to the unreactive $\text{Fe}(\text{H}_2\text{O})_6^{3+}$.

The difference between the two solvents can be rationalized by changes in redox thermodynamics of iron and acid-base chemistry of superoxide, $\text{HO}_2^{\bullet}/\text{O}_2^{\bullet-}$, as follows. In both solvents the reaction between the substrate and active oxidant, an iron(IV) species, takes place in parallel one-electron (hydrogen-atom abstraction) and two-electron (hydride transfer) paths. The two-electron path is much more prominent in acetonitrile, presumably because it avoids the strongly oxidizing Fe(III) ($E = 1.6 \text{ V vs. NHE}$).⁸ This path regenerates the active catalyst, $\text{Fe}(\text{CH}_3\text{CN})_6^{2+}$, directly. The parallel hydrogen atom transfer produces carbon radicals and Fe(III). The ensuing chemistry in the presence of O_2 generates superoxide ($E^0(\text{O}_2/\text{O}_2^{\bullet-}) = -0.80$

V vs. NHE)³⁰ which rapidly reduces Fe(III) to Fe(II). This step both regenerates the catalyst and removes O₂^{•-}, the key intermediate involved in chain decomposition of ozone.

The two paths are of comparable importance in acidic aqueous solutions¹ so that a substantial portion of Fe(H₂O)₆²⁺ is oxidized to Fe(H₂O)₆³⁺ in a single cycle. Similar to the reaction in acetonitrile, the follow-up chemistry generates superoxide. However, under acidic conditions the superoxide is protonated (pK_a (HO₂[•]/ O₂^{•-}) = 4.69)³⁰ and incapable of reducing Fe(H₂O)₆³⁺. One-electron path in aqueous solution thus leads to irreversible removal of the catalyst.

Supporting Information Available: Figures S1-S21 and Tables S1-S3.

Acknowledgment. We are grateful to Dr. Jana for help with the synthesis of iron(II) bis(acetonitrile) complex. This research is supported by the U.S. Department of Energy, Office of Science, Basic Energy Sciences, Division of Chemical Sciences, Geosciences, and Biosciences through the Ames Laboratory. The Ames Laboratory is operated for the U.S. Department of Energy by Iowa State University under Contract DE-AC02-07CH11358.

References

- (1) Pestovsky, O.; Bakac, A. *J. Am. Chem. Soc.* **2004**, *126*, 13757-13764.
- (2) Pestovsky, O.; Stoian, S.; Bominaar, E. L.; Shan, X.; Münck, E.; Que, L. J.; Bakac, A. *Angew. Chem., Int. Ed.* **2005**, *44*, 6871-6874.
- (3) Jacobsen, F.; Holcman, J.; Sehested, K. *Int. J. Chem. Kin.* **1998**, *30*, 215-221.
- (4) Logager, T.; Holcman, J.; Sehested, K.; Pedersen, T. *Inorg. Chem.* **1992**, *31*, 3523-3529.
- (5) Pestovsky, O.; Bakac, A. *Inorg. Chem.* **2006**, *45*, 814-820.

- (6) Bataineh, H.; Pestovsky, O.; Bakac, A. *Chem. Sci.* **2012**, *3*, 1594-1599.
- (7) Kratochvil, B.; Long, R. *Analytical Chemistry* **1970**, *42*, 43-46.
- (8) Sugimoto, H.; Sawyer, D. T. *J. Am. Chem. Soc.* **1985**, *107*, 5712-5716.
- (9) Bakac, A.; Pestovsky, O.; Vol. U.S. Patent 8507730 (2013).
- (10) Hagen, K. S. *Inorganic Chemistry* **2000**, *39*, 5867-5869.
- (11) Leitzke, A.; von Sonntag, C. *Ozone: Sci. Eng.* **2009**, *31*, 301-308.
- (12) Franco, C.; Olmsted Iii, J. *Talanta* **1990**, *37*, 905-909.
- (13) Nimlos, M. R.; Wolfrum, E. J.; Brewer, M. L.; Fennell, J. A.; Bintner, G. *Environmental Science & Technology* **1996**, *30*, 3102-3110.
- (14) Hay, M. T.; Geib, S. J.; Pettner, D. A. *Polyhedron* **2009**, *28*, 2183-2186.
- (15) Avgousti, C.; Georgolios, N.; Kyriacou, G.; Ritzoulis, G. *Electrochimica Acta* **1999**, *44*, 3295-3301.
- (16) Klang, J. A.; Lawson, A. P.; ARCO Chemical Technology, L.P.: United States, 1993; Vol. US005254702A, p 1-4.
- (17) Suárez, A. R.; Rossi, L. I.; Martín, S. E. *Tetrahedron Letters* **1995**, *36*, 1201-1204.
- (18) Kirchner, K.; Kirchner, R.; Jedlicka, R.; Schmid *Monatshefte für Chemie* **1992**, *123*, 203-209.
- (19) Flyunt, R.; Leitzke, A.; Mark, G.; Mvula, E.; Reisz, E.; Schick, R.; von Sonntag, C. *The Journal of Physical Chemistry B* **2003**, *107*, 7242-7253.
- (20) Langlais, B.; Reckhow, D. A.; Brink, D. R. In *Am Water Works Res*; CRC press: 1991.
- (21) Gonzalez, M. C.; Mártire, D. O. *International Journal of Chemical Kinetics* **1997**, *29*, 589-597.
- (22) Gonzalez, M. C.; Mártire, D. O. *Water Science and Technology* **1997**, *35*, 49-55.
- (23) Naumov, S.; von Sonntag, C. *Environmental Science & Technology* **2011**, *45*, 9195-9204.
- (24) Rush, J. D.; Bielski, B. H. J. *The Journal of Physical Chemistry* **1985**, *89*, 5062-5066.
- (25) Nakano, Y.; Okawa, K.; Nishijima, W.; Okada, M. *Water Research* **2003**, *37*, 2595-2598.

- (26) Mitroka, S.; Zimmeck, S.; Troya, D.; Tanko, J. M. *Journal of the American Chemical Society* **2010**, *132*, 2907-2913.
- (27) Afanas'ev, I. B.; Kuprianova, N. S. *Journal of the Chemical Society, Perkin Transactions 2* **1985**, 1361-1364.
- (28) Singh, P. S.; Evans, D. H. *The Journal of Physical Chemistry B* **2005**, *110*, 637-644.
- (29) McCandlish, E.; Miksztal, A. R.; Nappa, M.; Sprenger, A. Q.; Valentine, J. S.; Stong, J. D.; Spiro, T. G. *Journal of the American Chemical Society* **1980**, *102*, 4268-4271.
- (30) Sawyer, D. T.; Valentine, J. S. *Accounts of Chemical Research* **1981**, *14*, 393-400.
- (31) Bielski, B. H. J.; Cabelli, D. E.; Arudi, R. L.; Ross, A. B. *J. Phys. Chem. Ref. Data* **1985**, *14*, 1041-1100.
- (32) Lind, J.; Merenyi, G.; Johansson, E.; Brinck, T. *J. Phys. Chem. A* **2003**, *107*, 676-681.
- (33) Gall, B. L.; Dorfman, L. M. *J. Amer. Chem. Soc.* **1969**, *91*, 2199-2204.
- (34) Buxton, G. V.; Greenstock, C. L.; Helman, W. P.; Ross, A. B. *J. Phys. Chem. Ref. Data* **1988**, *17*, 513-886.
- (35) DeMatteo, M. P.; Poole, J. S.; Shi, X.; Sachdeva, R.; Hatcher, P. G.; Hadad, C. M.; Platz, M. S. *J. Am. Chem. Soc.* **2005**, *127*, 7094-7109.
- (36) Sehested, K.; Holcman, J.; Bjergbakke, E.; Hart, E. J. *J. Phys. Chem.* **1987**, *91*, 2359-2361.
- (37) Batt, L. *Int. Rev. Phys. Chem.* **1987**, *6*, 53-90.
- (38) Kirillov, A. I. *Zh. Obshch. Khim.* **1966**, *2*, 1048-1052.
- (39) Kuntz, I. *J. Polym. Sci., Part B Polym. Lett.* **1966**, *4*, 427-430.
- (40) Martín, S. E.; Suárez, D. o. F. *Tetrahedron Letters* **2002**, *43*, 4475-4479.
- (41) Potapenko, E. V.; Andreev, P. Y. *Russian Journal of Applied Chemistry* **2010**, *83*, 1243-1247.
- (42) Fitzpatrick, P. F. *Biochemistry* **2003**, *42*, 14083-14091.
- (43) de Visser, S. P.; Oh, K.; Han, A.-R.; Nam, W. *Inorganic Chemistry* **2007**, *46*, 4632-4641.